

CONF-760816-25

LA-UR -76-892

TITLE: HEAT TRANSFER PROBLEMS ASSOCIATED WITH LASER FUSION

AUTHOR(S): T. G. Frank, I. O. Bohachevsky, L. A. Booth,
and J. H. Pendergrass

SUBMITTED TO: 16th National Heat Transfer Conference,
St. Louis, MO, August 8-11, 1976

By acceptance of this article for publication, the publisher recognizes the Government's (license) rights in any copyright and the Government and its authorized representatives have unrestricted right to reproduce in whole or in part said article under any copyright secured by the publisher.

The Los Alamos Scientific Laboratory requests that the publisher identify this article as work performed under the auspices of the USERDA.



An Affirmative Action/Equal Opportunity Employer

NOTICE
This report was prepared as an account of work sponsored by the United States Government. Neither the United States nor the United States Energy Research and Development Administration, nor any of their employees, nor any of their contractors, subcontractors, or their employees, makes any warranty, express or implied, or assumes any legal liability or responsibility for the accuracy, completeness or usefulness of any information, apparatus, product or process disclosed, or represents that its use would not infringe privately owned rights.

UNITED STATES
ENERGY RESEARCH AND
DEVELOPMENT ADMINISTRATION
CONTRACT W-7405-ENG-36

MASTER

HEAT TRANSFER PROBLEMS ASSOCIATED WITH LASER FUSION*
T. G. Frank, I. O. Bohachevsky, L. A. Booth, and J. H. Pendergrass
Los Alamos Scientific Laboratory, Los Alamos, New Mexico 87545

Abstract

Briefly discussed are the laser-initiated fusion reaction, emissions that are produced, and methods that may be used to protect the walls of reactor cavities from these emissions. Thermal loadings encountered in laser fusion reactors will consist of energy deposition by discrete, short, intense pulses of x and gamma rays, fast alpha and other charged particles, and fusion neutrons. Presented are models of energy deposition in structural walls and blanket regions surrounding the reaction chamber and methods used to calculate resulting temperature increases and thermal stresses in these components. The results of such calculations indicate that the design conditions for the engineering of laser-initiated fusion reactors will be severe and a great amount of ingenuity and analysis will be required to meet them successfully.

I. INTRODUCTION

Laser-induced fusion is an attractive potential alternative and/or supplement to magnetically confined fusion for satisfying anticipated national and global energy needs. Fusion reactors are expected to be significant sources of consumable energy in the early part of the next century.

The development of laser-fusion technology is being paced by the time required to develop and construct high-power-level, short-pulse lasers. Significant numbers of thermonuclear neutrons have been produced by fusion pellet irradiations with laser power levels less than 1 TW. New and unprecedented lasers with power levels as large as 200 TW are scheduled for completion during the next five years. Achievement of scientific breakeven (thermonuclear energy release equal to laser energy input) is expected with this new generation of lasers.

The understanding of the physics of laser-induced fusion does not permit definitive specification of either fusion-pellet designs or properties of fusion microexplosions. Sophisticated calculational techniques to analyze laser-induced fusion have been developed but suffer from the lack of corroborating experimental data. Nevertheless, these calculations provide the best available data to identify the unique design requirements for laser fusion reactor (LFR) concepts.

Conceptual laser fusion reactors include a reaction chamber or reactor cavity in which fusion-pellet microexplosions are contained. Pellets containing fusion fuel are injected into the reactor cavity where they are illuminated by intense laser beams resulting in heating and compression of the fuel to conditions required for self-sustaining thermonuclear burn. The laser beams are reflected and/or focused by mirrors into the cavity through openings in the cavity wall. The fusion fuel in first-generation fusion reactors will consist of stoichiometric mixtures of deuterium and tritium (DT). Because of the necessity to breed tritium for the fuel cycle by neutron reactions with lithium, reactor cavities are surrounded by relatively thick blanket regions containing lithium or lithium compounds.

The major problems encountered in the containment of fusion-pellet microexplosions and in analyzing energy deposition and recovery in LFRs are discussed in this paper. The characteristics of fusion pellet microexplosions are described in Section II and microexplosion containment alterna-

tives in Section III. Section IV consists of descriptions of energy deposition mechanisms in reactor cavities and blankets and of models for analyzing the unique heat-transfer problems that arise.

II. FUSION PELLETT MICROEXPLOSIONS

The physical and chemical form of the fuel for LFRs has not been determined; however, the most promising candidate is molecular DT in gaseous, liquid or solid form. Of equal importance, with regard to LFR concepts, is the encapsulating pellet material. The DT fuel might be simply frozen pellets of pure DT or it might be contained, for example, within a structural shell or system of shells. The use of bare frozen DT pellets is conceptually attractive, and a number of detailed calculations have been made of pure DT microexplosions (see, for instance, Clarke, et al. [1]).

In the process of heating and compressing bare fusion pellets with laser beams, material is ablated or blown off from the surface of the pellet (Booth, et al. [2]). The thermonuclear fuel is compressed and heated by the balance of momentum from the expanding (ablated) material. Recent investigations (Ehler, et al. [3]) indicated problems of low thermal conductivity and anomalously poor absorption of laser light. Very high energy ions are produced that carry away most of the energy but with insufficient momentum to adequately compress the thermonuclear fuel, thus indicating fundamental difficulties with bare spherical pellets. Accordingly, increased attention is being given to fusion pellet design variations and different coupling mechanisms using structured pellets in order to mitigate or avoid these difficulties.

Theoretical energy-release forms from ~ 100 -MJ pellet microexplosions are given in Table I (Henderson [4], Booth [5], Williams, et al. [6]). For the bare DT pellet, prompt x rays would be observed first. The 14-MeV neutrons would follow next in time, then high-energy (~ 2 -MeV) alpha particles, and finally the plasma of pellet debris. For structured pellets, the energy release mechanisms observed just outside the expanding pellet will depend on the thermonuclear yield and on the composition and mass of the structural container. A relatively massive shell of high atomic number will absorb the energy of the 3.5-MeV alpha particles released by (D+T) reactions and will, in turn, radiate x rays as a blackbody. The fractional

*Work performed under the auspices of the U.S. Energy Research and Development Administration, Contract Number W-7405-ENG-16.

TABLE I
 THEORETICAL ENERGY RELEASE FORMS FROM FUSION-PELLET MICROEXPLOSIONS

	<u>Bare (Frozen) DT</u>		<u>Structured Pellet</u>	
	<u>Fraction of Total Energy</u>	<u>Average Energy</u>	<u>Fraction of Total Energy</u>	<u>Average Energy</u>
Energy escaping pellet				
Photons	0.01	~ 4 keV peak	0.05	0.9 MeV
α Particles	0.07	~ 2 MeV	—	—
Neutrons	0.77	~ 14 MeV	0.70	12 MeV
Energy deposited in pellet	0.15	50 keV/particle	0.25	0.2 MeV/particle

energy release in x rays will be larger than for a bare pellet, but with a softer spectra. However, a higher-energy gamma-ray component will also be present due to neutron scattering reactions with the structural materials. Most of the 14-MeV neutrons will escape the pellet with slight degradation in energy.

The time scales associated with these events are important for estimating the responses of reactor components. The thermonuclear burn lasts ~ 10 ps and is terminated by expansion of the fusion fuel. Energy deposition in cavity and blanket components by x rays from pure DT microexplosions occurs in a time interval of this same magnitude. X and gamma radiation from structured pellets occurs over a somewhat longer time interval. Energy deposition by neutrons occurs primarily in blanket regions in neutron-slowing-down times, a few microseconds for 14-MeV neutrons in lithium. The arrival times at reaction chamber interfaces of free-streaming charged particles and of the debris plasma depend on chamber geometry and dimensions, on the kinetic energy and spectra of the particles, and are also affected by the presence of an ambient gas or a magnetic field in the reaction cavity. Time intervals for energy deposition by charged particles are of the order of a few microseconds for ~ 100 MJ microexplosions in reaction chamber concepts that have been analyzed.

Fusion-pellet-microexplosion repetition rates are important factors in determining the cost of producing power. Repetition rates of 1 to 10 per second appear feasible for reactor concepts being evaluated.

III. ALTERNATIVES FOR CONTAINMENT OF FUSION-PELLET MICROEXPLOSIONS

In a LFR, fusion-pellet microexplosions must be contained in a manner that both prevents excessive damage to reactor components and permits recovery of the energy in a form suitable for utilization in an energy conversion cycle. Energy deposition by x rays, free-streaming charged particles, and particles in the debris plasma occurs at, or very near, surfaces of incidence in structural and coolant materials; the energy of 14-MeV neutrons and high-energy gamma rays is deposited throughout relatively large material volumes.

A bare cavity wall (e.g., a bare refractory metal) would be the simplest reactor cavity enclosure. However, the interior wall of such a cavity would have to withstand repeated energy deposition amounting to 20-30% of the thermonuclear yield within a few micrometers of its surface, and unless very large cavities were used, very high surface temperature increases would result. Tolerable surface temperature increases of such structural components have not been established either by

theory or experiment, but it is probably expedient to design systems that at least prevent temperature excursions from exceeding the melting point of the wall material. For a cavity made of niobium, this constraint would result in a minimum cavity diameter of about 12 m to contain the 100-MJ pure-DT microexplosion described in Table I. There are economic incentives for reducing the cavity diameter below this value. One solution might be to operate with the highest permissible ambient gas density, allowing a spherical blast wave to develop. Calculations show, however, that the blast heated gas would only reside at the chamber wall for a very short time--too short for sufficient thermal conduction into the wall. Steady-state operation with repeated fusion-pellet microexplosions would result in a very turbulent, hot cavity medium with energy transport to the chamber walls by radiation and thermal conduction, complicating pellet injection and illumination by laser beams.

There are several reactor cavity concepts that employ evaporative and/or ablative materials to protect interior cavity wall surfaces. For such concepts, it is necessary that the protective material be renewable between pellet microexplosions, otherwise cavity wall lifetimes would be uneconomically short. Protection of exposed surfaces by a liquid metal such as lithium has many attractive features and is utilized in the wetted-wall concept proposed by the Los Alamos Scientific Laboratory (Booth[5], Williams, et al.[6], Williams, et al.[7]) and the suppressed ablation concept proposed by the Lawrence Livermore Laboratory (Hovingh, et al.[8]).

Externally applied magnetic fields in a cylindrical cavity could be used to divert charged particles out the ends of the cylinder leaving only the x-ray energy to be accommodated by the cavity wall surface. This approach is also being exploited by the Los Alamos Scientific Laboratory (Frank, et al.[9]). Central energy-sink surfaces are placed in the ends of the cylindrical cavity and the charged particles are incident on these surfaces

IV. HEAT TRANSFER IN LASER FUSION REACTORS

A. Energy Deposition and Heat Transfer in Cavity Walls. The most challenging engineering problems encountered in LFR design are associated with protection of the surfaces of cavity components from damage due to x rays and energetic charged particles. Energy deposition densities in cavity walls due to neutrons and gamma rays are not large by conventional standards and do not pose significant problems.

X Rays. Depending on the pellet design and constituents, a wide range of x-ray spectra are possible from fusion pellet microexplosions. A typical x-ray spectrum from a 100-MJ, pure DT microexplosion is shown in Fig. 1. X-ray spectra

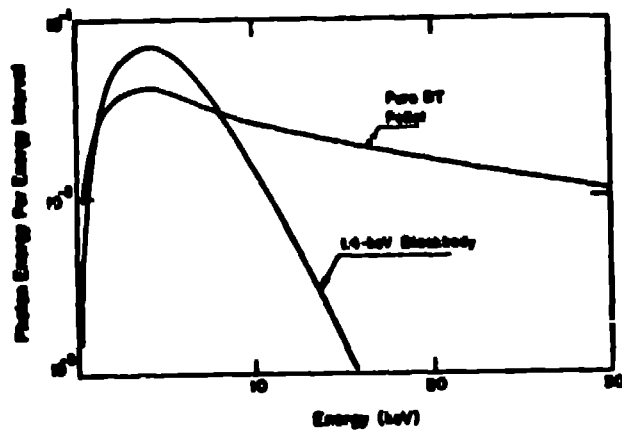


Figure 1. X-ray spectrum from 100-MJ pure DT fusion-pellet microexplosion with blackbody spectrum for comparison.

from structured pellets containing high atomic number materials are expected to have a Planck blackbody distribution but the blackbody temperature will depend on the yield, mass and composition of the pellet. It is important that surface temperature fluctuations for cavity components be estimated with reasonable accuracy since they determine minimum cavity dimensions for most reactor concepts.

Monte Carlo photon transport codes are used to calculate x-ray energy deposition for complex absorber geometries; however, many practical problems in LFR design involve relatively simple geometries for which somewhat less detailed analyses are appropriate. Exponential decay laws with sufficiently detailed treatment of x-ray scattering processes have been found to reproduce detailed Monte Carlo results with acceptable accuracy for simple geometries. A computer program (Gardner and Seitz[10]) is used which sums the contributions from photoelectric capture, coherent scattering, and incoherent (Compton) scattering. Pair production is not included because the applications involve x-ray energies below the threshold for this type of interaction.

Scattered photons are assumed to have azimuthal symmetry relative to the incident beam. An approximate angular distribution of the scattered fluence is calculated by dividing the scattering directions into conical sectors subtending finite polar angles, θ , as illustrated in Fig. 2. Secondary scattering, i.e., scattering from one conical sector into another, is approximated by assuming the same type of symmetry as in the primary beam scattering. Backscattering is accounted for by lumping all backscattered radiation into the opposite direction relative to the primary beam.

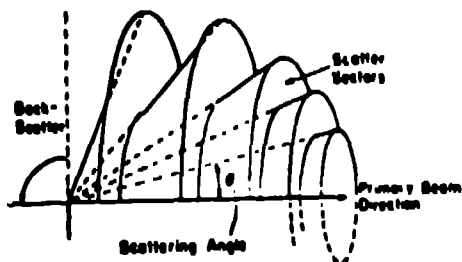


Figure 2. Schematic representation of x-ray scattering sectors.

Comparisons have been made between the results of Monte Carlo calculations and the approximation described above for a number of absorber configurations, including some in which geometry-dependent scattering losses were significant. Generally, the agreement is within 5% for intermediate or high atomic number materials but discrepancies as large as 10 to 15% may occur for low atomic number materials.

Surface temperature increases due to x-ray deposition in materials of interest for cavity wall construction (i.e., refractory metals and stainless steels) are very large. However, temperature fluctuations are diminished considerably by protective layers of materials with low atomic number that filter out the low-temperature components of the spectrum. Liquid lithium is useful for this purpose since it is easily renewable between microexplosions and also affords protection from energetic charged particles emanating from pellet microexplosions. Protective layers of carbon and metal carbides are also utilized in some reactor cavity concepts. The effectiveness of thin layers of lithium and carbon to protect niobium components from the pure DT-pellet x-ray spectrum given in Fig. 1 are shown in Fig. 3. Protection of metal surfaces from the relatively low-temperature x-ray spectra from structured pellets is more crucial than for the pure-DT-pellet spectrum. Stainless steel surface temperature increases with and without a protective lithium layer are shown in Fig. 4 as functions of blackbody temperature.

Pre-streaming charged particles and pellet debris plasma. Protection of cavity component surfaces from impinging charged particles can be achieved by restorable protective layers, by diversion with magnetic fields, or by providing large surface areas so that the fluence per unit area is small.

For cavity concepts with restorable protective layers, such as liquid lithium, the energy of the charged particles is deposited in depths of a few micrometers from the surface. This surface material is evaporated and ablated into the cavity interior from which it is exhausted through a nozzle into a condenser and heat exchanger.

In cavity concepts that are based on the use of magnetic fields to deflect charged particles away from cavity walls, the particles are incident on "energy sinks" which have large surface areas consisting of carbon, a metal carbide, or some other

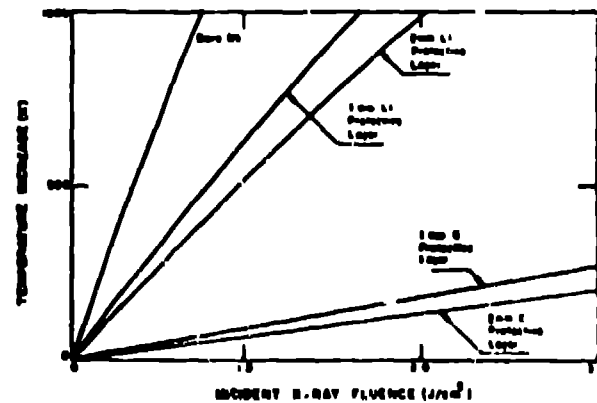


Figure 3. Niobium surface temperature increases due to instantaneous deposition of x rays from pure DT pellet microexplosion for bare and protected spheres.

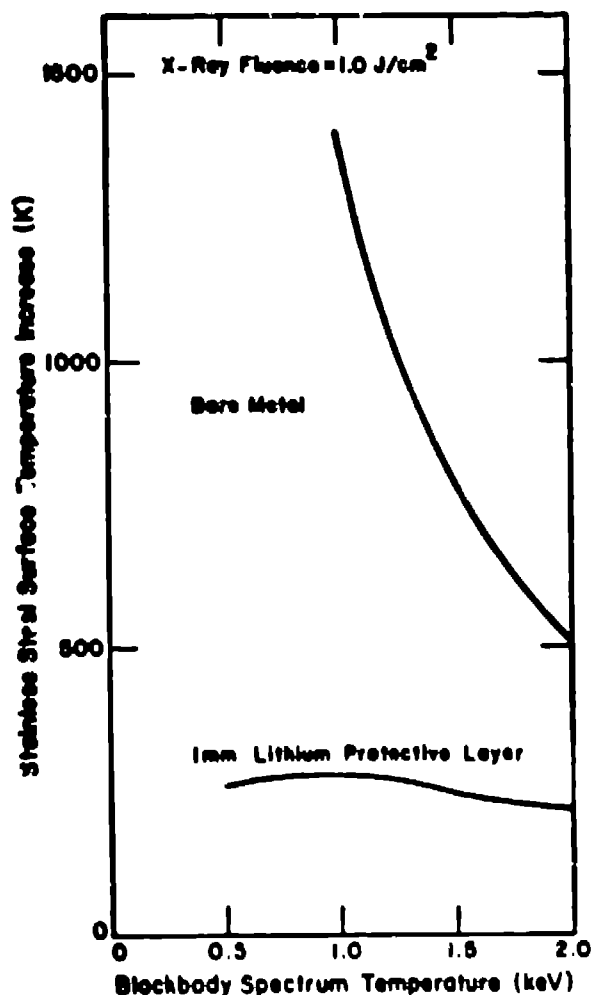


Figure 4. Stainless steel surface temperature increases due to instantaneous deposition of blackbody spectrum of x rays for bare and protected surface.

refractory material. Energy sink surface lifetimes are determined by the rate at which they are eroded or evaporated. Thus, design criteria include limits on surface temperature fluctuations. The time intervals of arrival of charged particles at the energy sinks are long compared to other pellet emissions and significant conduction of heat away from the surface can take place during deposition. Particle fluxes may consist of discrete lines of different types of particles and with different energy spectra. Particle ranges in energy sink surface materials of interest will depend on particle type and energy and on the surface material but will generally be less than about 100 μm.

The problem of calculating the surface temperature increase of the energy sinks can be modeled mathematically in at least two ways. A surface flux model is described by the equation

$$\frac{\partial T}{\partial t} = \kappa \frac{\partial^2 T}{\partial x^2} \quad (1)$$

and the boundary condition

$$-\kappa c \rho \frac{\partial T}{\partial x} = F \text{ at } x = 0, \quad (2)$$

where: T is temperature, t is time, x is space coordinate perpendicular to the surface, κ is thermal diffusivity, ρ is density, c is heat capacity,

and F is flux of energy per unit surface area per unit time. Alternatively, a volume source model may be used which is described by the equation

$$\frac{\partial T}{\partial t} = \kappa \frac{\partial^2 T}{\partial x^2} + \frac{S}{\rho c} \quad (3)$$

and the boundary condition

$$\frac{\partial T}{\partial x} = 0 \text{ at } x = 0 \quad (4)$$

where S is the rate of energy deposition per unit volume per unit time.

The surface temperature increase at the end of a uniform pulse of duration τ predicted by the surface flux model is well known (see for instance Carslaw and Jaeger[1]) to be

$$T_A(0, \tau) = \frac{2F}{\rho c \sqrt{\pi \kappa}} \sqrt{\tau} \quad (5)$$

This solution has frequently been used (Craston, et al.[12], Behrish[13]) to calculate first wall evaporation rates in magnetically confined fusion reactors.

The surface temperature increase predicted by the volume source model has been determined for a single square pulse of duration τ to be (Anford[14])

$$T_B(0, \tau) = \frac{S_0 \tau}{\rho c} \left[\text{erf } u - 2u^2 \text{erfc } u + \frac{2}{u} u e^{-u^2} \right] \quad (6)$$

where the volume source is given by

$$S = \begin{cases} S_0, & 0 < t \leq \tau, \quad 0 \leq x \leq \delta \\ 0, & \text{otherwise} \end{cases}$$

$S_0 = \text{constant}$
 $\delta = \text{depth of energy deposition}$
 $u = \delta / (2\sqrt{\kappa \tau})$

The two solutions can be compared for the same thermal loading by requiring

$$F = S_0 \delta. \quad (7)$$

Comparisons of temperature increases predicted for stainless steel by Equations (5) and (6) are shown in Fig. 5 for $F = 10^7 \text{ J/cm}^2 \cdot \text{s}$ and $\delta = 5 \mu\text{m}$. The plots illustrate the different behavior of the two solutions for short pulses. The surface flux model predicts that the surface temperature will increase as $\tau^{1/2}$ and the volume source model predicts that it will approach the value $F/\rho c \delta$, which is constant for fluxes inversely proportional to pulse durations.

Comparisons between the two models can be generalized by recognizing that for some applications in LFR design, u is numerically small. For such cases, T_B (Eq. 6) can be expanded in powers of u from which the ratio

$$\frac{T_A(0, \tau)}{T_B(0, \tau)} = 1.0 + O(u) \quad (8)$$

can be obtained. Thus, for small u, the results from the two models will be in substantial agreement. The nondimensional variable u is a measure of the "surface effect" or "skin depth" (see, for example, Behrish[13], Fig. 6).

The fractional difference between surface temperatures calculated from the two models is shown in Fig. 6 as a function of u. The dependence is almost linear and the constant of proportionality is nearly unity.

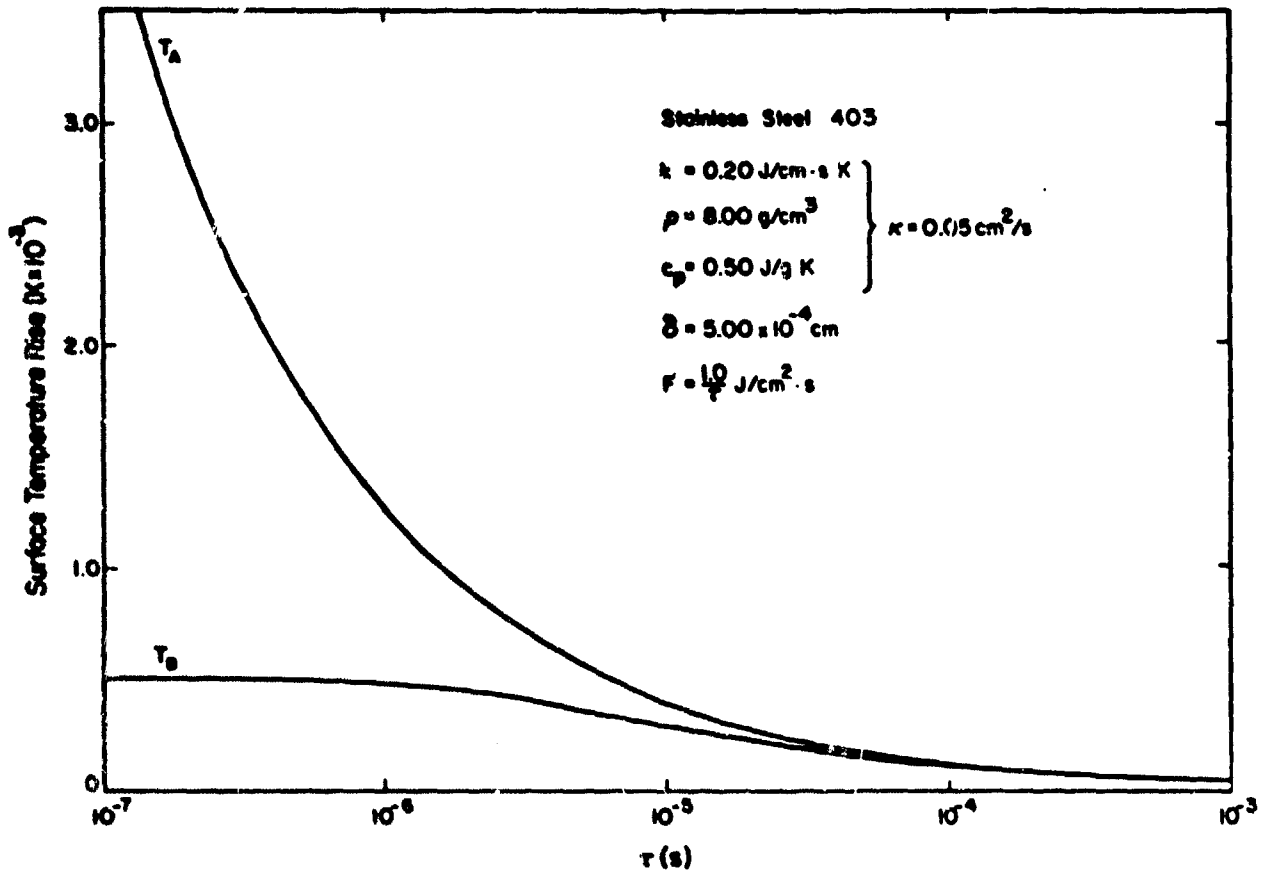


Figure 5. Surface temperature rise for stainless steel calculated with the surface flux (T_A) and volume source (T_B) models.

Present estimates of energy deposition by charged particles in LFRs indicate thermal loadings consisting of several pulses, some of which overlap in time and are short enough to fall in the regime where surface flux models are not sufficiently accurate. To cope with this situation, the volume source model (Eq. 3) has been generalized to include a source, S , consisting of the superposition of an arbitrary number of pulses:

$$S = \sum_{i=1}^N S_i \quad (9)$$

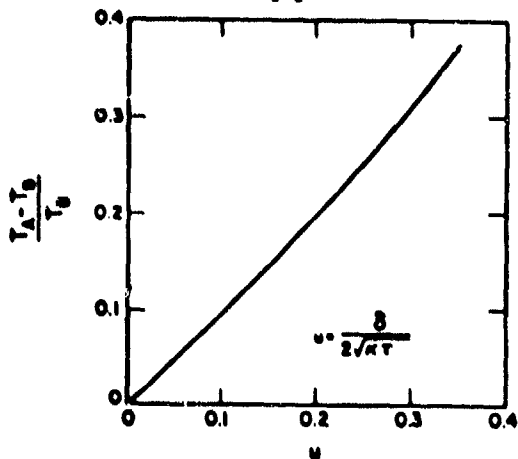


Figure 6. Normalized difference between surface temperature rises obtained from surface flux and volume source models.

with

$$S_i = S_{oi} \text{ for } 0 \leq x \leq \delta_i, t_{i1} < t < t_{i2}$$

$$S_i = 0 \text{ otherwise.}$$

An example of two nonoverlapping pulses is illustrated schematically in Fig. 7.

A general solution of this problem has been obtained using Laplace transform techniques and is expressed explicitly in terms of parabolic cylinder functions. The resulting expressions are too lengthy to be included in full generality in the present paper and will be published elsewhere.

Here the solution is illustrated by an example of the surface temperature response to two pulses incident on molybdenum as shown in Fig. 8. The first pulse is 0.1 μ s long, penetrates to a depth of 5.8 μ m, and has a source strength of 6×10^{10} J/cm²-s. The second pulse begins 0.5 μ s after termination of the first pulse, lasts for 0.6 μ s, penetrates to a depth of 0.677 μ m, and has a source strength of 1.71×10^{10} J/cm²-s. This solution clearly shows the cooling between the pulses and the rapid temperature decrease at the end of the second pulse due to the relatively good thermal conductivity of molybdenum. The temperatures predicted by the surface flux model at the end of each pulse are also indicated. As expected, for the first pulse, for which $u = 1.41$, the two predictions are very far apart. For the second pulse, $u = 0.07$, and the fractional surface temperature difference is about 92, consistent with the result presented in Fig. 5. Shown in Fig. 9 are the temperature distributions inside the wall corresponding to the surface temperature history

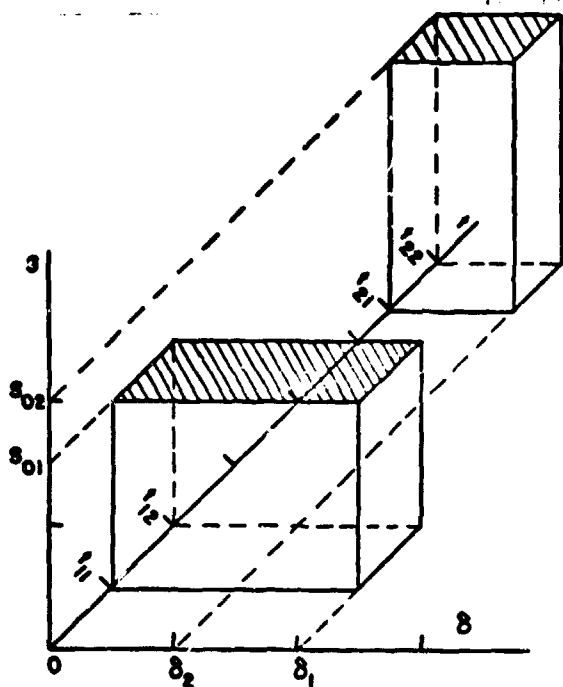


Figure 7. Volume source of two pulses.

presented in Fig. 8. Use of the above generalized formulation permits modeling of energy deposition and resulting surface and volume temperature variations due to penetrating radiation and energetic particles in any degree of detail desired. Non-uniform volume energy deposition can be approximated by successive pulses with appropriately different volume sources.

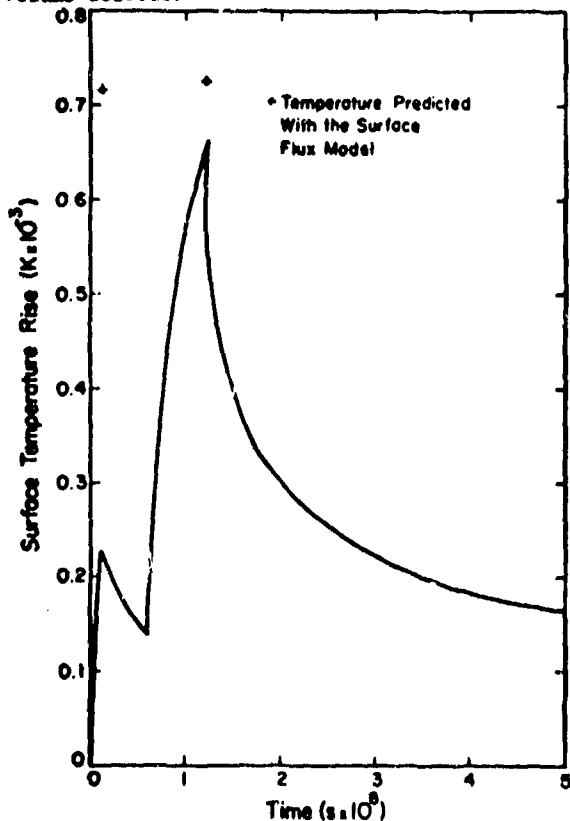


Figure 8. Surface temperature rise in response to two pulses.

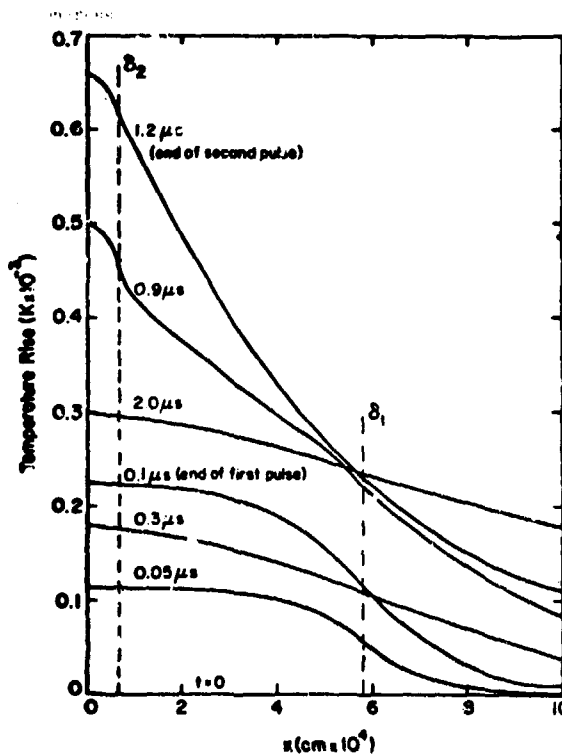


Figure 9. Temperature distributions inside the cavity wall caused by thermal loading of two pulses.

B. Energy Deposition and Heat Transfer in Reactor Blanket Regions

Reactor blankets have not been designed in detail; however, analyses have been made for conceptual designs in which circulating lithium is contained between structural shells enclosing the reactor cavity. The most detailed analyses of LFR blankets have been performed for spherical systems.

Neutron energy is deposited primarily in the liquid lithium by neutron scattering and exoergic capture reactions. Neutron capture reactions in structural components result in a substantial secondary gamma-ray source that is attenuated mainly by the structural shells. Cold lithium coolant flows to the lithium surrounding the porous cavity wall where it is divided. A small part of the flow is directed inward to replenish the protective film on the cavity wall interior between pellet microexplosions and the major part is directed radially outward for removal of the neutron and gamma-ray energy that is deposited in the blanket region.

Reactors that have been designed for minimum structural mass and acceptable tritium breeding ratios include three structural shells surrounding the reaction cavity. Neutron-energy deposition in liquid-lithium regions results in heating and expansion of the lithium. Because energy deposition in the lithium has a radial gradient and deposition times are very short ($\approx 10^{-6}$ s) compared to shell natural frequencies ($\approx 10^{-3}$ s), pressure waves result that travel between structural components. The shells respond to impulsive loads by ringing at essentially their natural frequencies, modified by the hydrodynamic coupling to the liquid lithium regions. Pulsed energy deposition in the structural shells results in thermal gradients which, in turn, give rise to thermal expansion and thermal stresses. Thus, reactor blankets must be designed

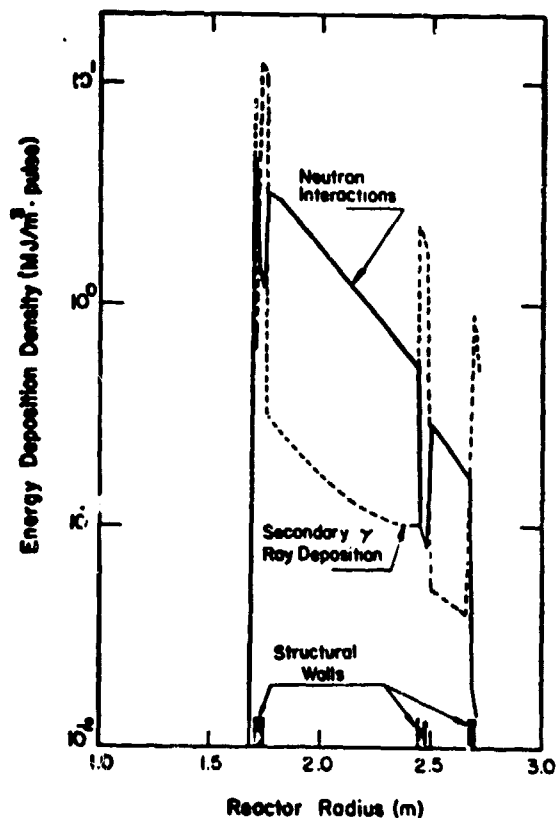


Figure 10. Neutron and gamma ray energy deposition inside a 1-m-thick lithium blanket.

to withstand repeated stresses due to the cyclic nature of LFR operation.

Neutron and gamma-ray energy deposition distributions from 100-MJ pure DT microexplosions are shown in Fig. 10 in a 1-m-thick blanket surrounding a 1.7-m-radius cavity. The innermost structural shell is loaded not only by the pressure waves in the lithium but also by the recoil momentum from the ablation of lithium from the interior of the cavity wall. Structural shell thicknesses have been calculated to contain 100-MJ pellet microexplosions for either niobium, molybdenum, or stainless steel at temperatures up to 1000 K. The ringing hoop stresses for the innermost structural shell are shown in Fig. 11.

Start-up analyses have been performed for the reactor with a 1-m-thick blanket surrounding a 1.7-m-radius cavity for a 100-MJ pellet microexplosion repetition rate of one per second. The results indicate that because of the large heat capacity of the system, the perturbations due to individual pulses are hardly discernable. Equilibrium blanket temperature distributions are achieved after about 300 microexplosions and are shown for three different lithium flow rates in Fig. 12.

V. SUMMARY AND CONCLUSIONS

Although as yet an unproven technology, laser fusion offers an attractive potential source of commercial power. The most critical unsatisfied technology requirements are those related to achieving significant fusion-pellet burn. Detailed engineering of reactor designs must await confirmation of fusion-pellet design and microexplosion characteristics. Laser systems with power levels exceeding 100 TW are scheduled for operation within the next few years and are expected to enable the

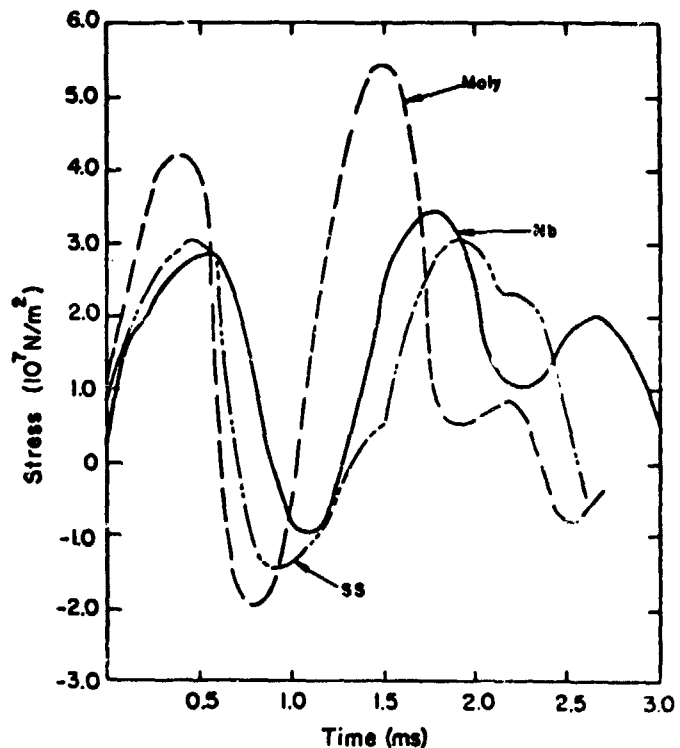


Figure 11. Hoop stresses in innermost structural shell of spherical laser fusion reactor as a function of time after pellet microexplosion.

achievement of the major milestone of scientific breakeven. With the achievement of this milestone, the laser-fusion program would proceed from the research to the technology development phase aimed at demonstrating the attractiveness of commercial operation.

The practical feasibility and preliminary engineering design of conceptual LFRs are being

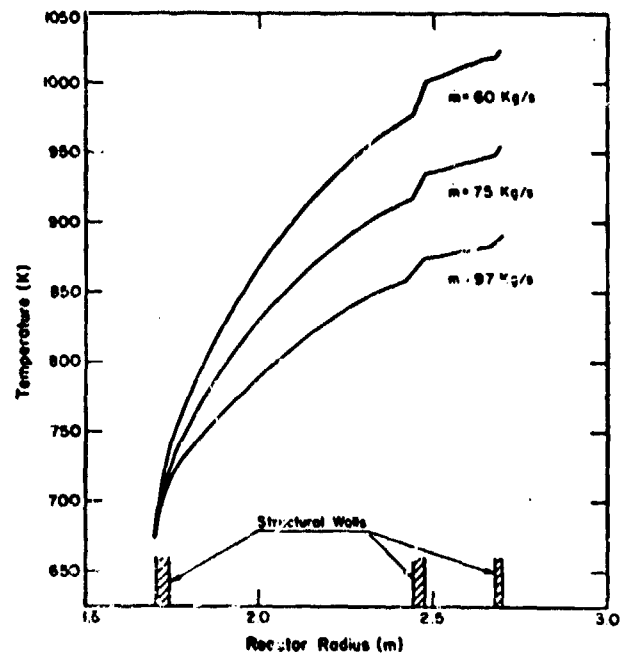


Figure 12. Equilibrium temperature distributions in the blanket of a spherical laser fusion reactor for different lithium coolant flow rates.

assessed based on theoretical predictions of fusion-pellet microexplosion emissions. Pellet microexplosions must be contained in a manner that both prevents excessive damage to reactor components and permits recovery of the energy in a form suitable for utilization in an energy conversion cycle. Optimization of reactor designs for minimum capital and operating costs have required the development of new engineering concepts to cope with unique problems of recovery and transfer of short intense bursts of energy in nonconventional forms.

The most hostile environment in a LFR results from the fusion-pellet microexplosion in the reactor cavity. In this paper some of the heat-transfer problems related to the conceptual design and analysis of LFR cavities have been identified, new methods for their solution indicated, and the results presented. These results indicate that the engineering problems associated with the development of LFRs will pose a formidable but not an insurmountable challenge.

Heat-transfer problems in laser-fusion generating stations other than those discussed in this paper include the cooling of very large mirrors and windows that will be exposed to intense short-pulse laser beams and possibly to radiation from the reactor cavity, and the cooling of high-repetition-rate low temperature laser power amplifiers.

REFERENCES

1. J. S. Clarke, H. N. Fisher and R. J. Mason, "Laser-Driven Implosion of Spherical DT Targets to Thermonuclear Burn Conditions," *Phys. Rev. Lett.* **30**, p. 89, January 15, 1973.
2. L. A. Booth, D. A. Freiwald, T. G. Frank and F. T. Finch, "Prospects of Generating Power with Laser-Driven Fusion," *Proc. of the IEEE*, to be published.
3. A. W. Ehler, D. V. Giovanielli, R. P. Godwin, G. H. McCall, R. L. Morse and S. D. Rockwood, "Evidence of Anomalously Reduced Thermal Conduction in Laser Produced Plasmas," Los Alamos Scientific Laboratory report LA-5611-MS (August 1975).
4. D. B. Henderson, Los Alamos Scientific Laboratory, unpublished work.
5. L. A. Booth (compiler), "Central Station Power Generation by Laser-Driven Fusion," Los Alamos Scientific Laboratory report LA-4858-MS, Vol. I (February 1972).
6. J. M. Williams, F. T. Finch, T. G. Frank and J. S. Gilbert, "Engineering Design for Laser Controlled Thermonuclear Reactors," *Proc. of 5th Symposium on Engineering Problems of Fusion Research*, Princeton, NJ (November 6-9, 1973).
7. J. M. Williams, T. Merson, F. Finch, F. Schilling and T. Frank, "A Conceptual Laser Controlled Thermonuclear Reactor Power Plant," *Proc. of 1st Topical Meeting on the Technology of Controlled Nuclear Fusion*, CONF-740402-P1, p. 70, San Diego, CA (April 16-18, 1974).
8. J. Hovingh, J. Maniscalco, M. Peterson and R. Werner, "The Preliminary Design of a Suppressed Ablation Laser-Induced Fusion Reactor", *Ibid.*
9. T. Frank, D. Freiwald, T. Merson and J. Devaney, "A Laser Fusion Reactor Concept Utilizing Magnetic Fields for Cavity Wall Protection," *Ibid.*
10. S. D. Gardner and W. L. Seitz, "HEX: A One-Dimensional Code for Computing X-Ray Absorption," Los Alamos Scientific Laboratory report LA-5114 (February 1973).
11. H. S. Carslaw, and J. C. Jaeger, "Conduction of Heat in Solids," 2nd edition Oxford Univ. Press, 1959, p. 57.
12. J. L. Craston, R. Hancox, A. E. Robson, S. Kaufman, H. T. Miles, A. A. Ware, and J. A. Wesson, "The Role of Materials in Controlled Thermonuclear Research," *Proc. 2nd Intl. Conf. Peaceful Uses of Atomic Energy*, **32** p. 414 (1958).
13. R. Behrish, "First-Wall Erosion in Fusion Reactors," *Nucl. Fusion* **12**, 695 (1972).
14. R. A. Axford, "Direct Evaluation of Transient Surface Temperatures and Heat Fluxes," Los Alamos Scientific Laboratory report LA-6031 (December 1975).